Journal of African Earth Sciences 162 (2020) 103689

Contents lists available at ScienceDirect

Journal of African Earth Sciences

journal homepage: www.elsevier.com/locate/jafrearsci

Probabilistic seismic hazard maps for South Africa

Vunganai Midzi*, B. Manzunzu, T. Mulabisana, B.S. Zulu, T. Pule, S. Myendeki

Council for Geoscience, 280 Pretoria Street, Silverton, Pretoria, South Africa

ARTICLE INFO

Keywords:
Seismic hazard assessment
South Africa
Source zones
GMPEs
OPENQUAKE
Earthquake catalogue

ABSTRACT

Many years have passed since previous national seismic hazard maps were prepared for South Africa. In those maps, zone-less techniques were applied. The availability of more reliable seismicity and geological data has made it possible to update those maps using probabilistic seismic hazard analysis methodologies that take into consideration all available data. This paper presents a summary of the work conducted to produce the latest seismic hazard maps for South Africa. This involved the systematic compilation and homogenisation of an earthquake catalogue, which comprised both historical and instrumental events. The catalogue played a prominent role in the preparation and characterisation of the seismic source model. Two ground motion prediction equations were identified from available international models for regions that are tectonically similar to South Africa. These two models were then implemented in the hazard calculations, which were done using the OPENQUAKE software. Uncertainties associated with input parameters in both the seismic source and ground motion models were taken into account and implemented using the logic tree technique. Maps showing distribution of acceleration at three periods (0.0s, 0.15s and 2.0s) computed for 10% probability of exceedance in 50 years were produced.

1. Introduction

The effects of earthquakes continue to have disastrous impact on the lives of people all over the world. Only in the last few years, catastrophic events hit Indonesia, China, Haiti, Chile and Japan resulting in over 600 000 casualties and dramatic economic consequences. These earthquakes have revealed how significant the implications of natural disasters for the economic productivity of whole regions are, up to devastating effects on large segments of the population, especially in poor countries. The Haiti earthquake of 12 January 2010 (M_w7.0) left over 200 000 people dead and up to a million homeless (International Federation of Red Cross and Red Crescent Societies report, 2010). This shows that seismic risk is increasing sharply in developing countries, mainly due to rapid population growth, urbanisation, lack of building codes, poor construction practice and failure to regulate construction. An improvement in risk identification, assessment and management in countries especially affected by seismic hazard and by a severe degree of vulnerability in terms of population and economic exposure is highly desirable.

Though South Africa is located in a stable continental region (SCR, Johnston et al., 1994), several moderate to large earthquakes have occurred in the country with the largest recorded being the Ceres, 29 September 1969 event of magnitude M_W6.2. This event resulted in the deaths of 12 people and damage to property worth millions of dollars (Fig. 1).

Several studies on the seismic hazards of South Africa were conducted over time (e.g. Fernández and Guzman, 1979; Shapira and Fernández, 1989; Midzi et al., 1999; Kijko et al., 2003). Fernández and Guzman (1979) published the first perceived seismic hazard map that depicted hazard levels in South Africa based on the distribution of annual extreme values. A subsequent study by Shapira and Fernández (1989) used the ‘direct approach’, which is a method to estimate the probability that a defined peak ground acceleration (PGA) will be exceeded at a specified location. The methodology is described by Shapira (1981, 1983) and Oman et al. (1984). In their study, Shapira and Fernández (1989) estimated the probability that a defined horizontal PGA will be exceeded at fourteen cities in southern Africa. The “Seismic Hazard Maps for Southern Africa” poster was published in 1992 by Fernández and du Plessis (1992). The poster comprised three maps: a map of hazard in terms of reported Modified Mercalli Scale intensities for the period between 1620 and 1988; a map showing PGA with a 10% probability of exceedance in 50 years; and a map of past South African seismicity. During the 1990s, the Global Seismic Hazard Assessment Programme (GSHAP) compiled and published a seismic hazard map for

* Corresponding author.
E-mail addresses: vmidzi@geoscience.org.za (V. Midzi), bmanzunzu@geoscience.org.za (B. Manzunzu), tmulabisana@geoscience.org.za (T. Mulabisana), bzulu@geoscience.org.za (B.S. Zulu), tuple@geoscience.org.za (T. Pule), smyendeki@geoscience.org.za (S. Myendeki).

https://doi.org/10.1016/j.jafrearsci.2019.103689
Received 3 May 2019; Received in revised form 25 October 2019; Accepted 26 October 2019
Available online 31 October 2019
1464-343X/

Fig. 1. Damage to dwellings in the Ceres area caused by the 29 September 1969, M_w6.2 earthquake (Image obtained from Pule et al., 2015).

the whole world (Giardini et al., 1999). South Africa was also included in the GSHAP as part of the hazard map for Africa (Midzi et al., 1999). However, only four broad seismic source zones were delineated for the whole country, which is not the proper representation for the seismicity and seismotectonics of South Africa. The last map prepared for South Africa was done by Kijko et al. (2003) and that map is included in Part 4 of the South African National Standard (SANS 10160-4:2011 - Seismic actions and general recommendations for building). They applied a parametric-historical approach, which does not take into account seismic source zones (Kijko et al., 2003; Kijko and Graham, 1998, 1999).

The results of all these earlier studies clearly show the earthquake hazard to which African countries are exposed. In some of the studies, especially those focussing on South African seismic hazard, the authors mainly considered the spatial distribution and sizes of earthquakes in the region. Alternative methodologies that are currently being implemented in recent initiatives such as the Global Earthquake Model (GEM), highlight and call for detailed region-oriented efforts that consider seismic sources (e.g., fault and area sources) in understanding and mapping the hazard due to earthquakes. Given that seismic hazard analysis is a dynamic process, which requires regular updates as new datasets become available, it was necessary that a new analysis be conducted for South Africa. The work conducted in this study was done by taking into account available tectonic, seismic and stress field data, following a probabilistic seismic hazard analysis (PSHA) methodology (Field et al., 2003; McGuire, 2004; USNRC, 2012) to update the seismic hazard maps of South Africa.

2. Tectonic setting of South Africa

Southern Africa is generally classified as a SCR (Johnston et al., 1994), bounded to the northeast by the East African Rift System (EARS). Although this structure is not well defined in southern Africa, it is linked to much of the seismicity in Mozambique, Zimbabwe, Zambia, Botswana, Namibia and South Africa. The basement geology of the region is dominated by Archean cratons and mobile belts (Fig. 2). The Kaapvaal and Zimbabwe Cratons are the oldest tectonic regions in southern Africa and form part of the Kalahari Craton, an Archean domain (Johnston et al., 1994) formed between 2.7 and 3.7 Ga covering an area of about 1.2 million km^2 (Adams and Nyblade, 2011). According to de Wit and Ransome (1992), the Kaapvaal Craton collided with the Zimbabwe Craton along the Limpopo Mobile Belt during the late Archean, which caused dominant foliation in the Zimbabwe Craton. Located to the northwest of the Kaapvaal Craton is the Kheis Mobile Belt (Fig. 2), which was indicated by Cornell et al. (2011) as possibly either an orogenic belt (~1800 Ma) or a northern branch of the Namaqua-Natal Belt (~1200 Ma), which is described as a thin-skinned region with east-verging thrust belt characteristics.

The southern margin of the Kaapvaal Craton is bounded by the Neoproterozoic Namaqua-Natal Belt, whereas the north-western margin is bounded by the Proterozoic Damara-Lufilia domain (e.g. Johnston et al., 1994). The Namaqua sector of the Namaqua-Natal Belt is separated on its north-eastern boundaries from the Kaapvaal Craton by the Paleoproterozoic Kheis belt (e.g. Adams and Nyblade, 2011). The Namaqua Mobile Belt extends north-west into Namibia where it forms a 'triple junction' with the Damara and Kaoko Mobile Belts in central Namibia. The Damara Mobile Belt itself appears to be part of a westward extension of the EARS through the Zambezi valley and the Okavango delta, both of which are associated with major earthquakes.

The Cape Fold Belt is a dominant structural domain along the southern African coast and is assumed to have been caused by late Palaeozoic compression associated with the assemblage of Pangea (Hälbich, 1983). According to Tucholke et al. (1981), the belt extends southwards offshore as far as the Agulhas Bank along the strike slip margin of south-eastern Africa. Along the eastern part of the Cape Fold Belt is a large duplex structure, formed along the southern margin of Gondwana (Booth et al., 2004). This duplex structure, formed during the Late Palaeozoic, contains typical patterns of numerous north-verging thrust faults and associated folds.

3. Earthquake catalogue

A critical input in all seismic hazard assessments is a reliable and accurate catalogue of earthquakes. This is usually of use in several aspects of the assessments (e.g. source delineation, recurrence parameter calculations and M_{max} determination). Gane (1939) compiled one of the first catalogues for southern Africa, focussing his effort specifically on South Africa. Gane and Oliver (1953), Fernandez and Guzman (1979), and Brandt et al. (2005) updated the catalogue as the years went by and new events were recorded. Mangongolo and Hutchins (2008) compiled an earthquake catalogue of Namibia whilst Malephane (2007) compiled the Lesotho catalogue as part of her study of the seismic hazard of Lesotho. Turyomurugyendo (1996) compiled the first homogeneous catalogue that covered the whole of southern and eastern Africa, which

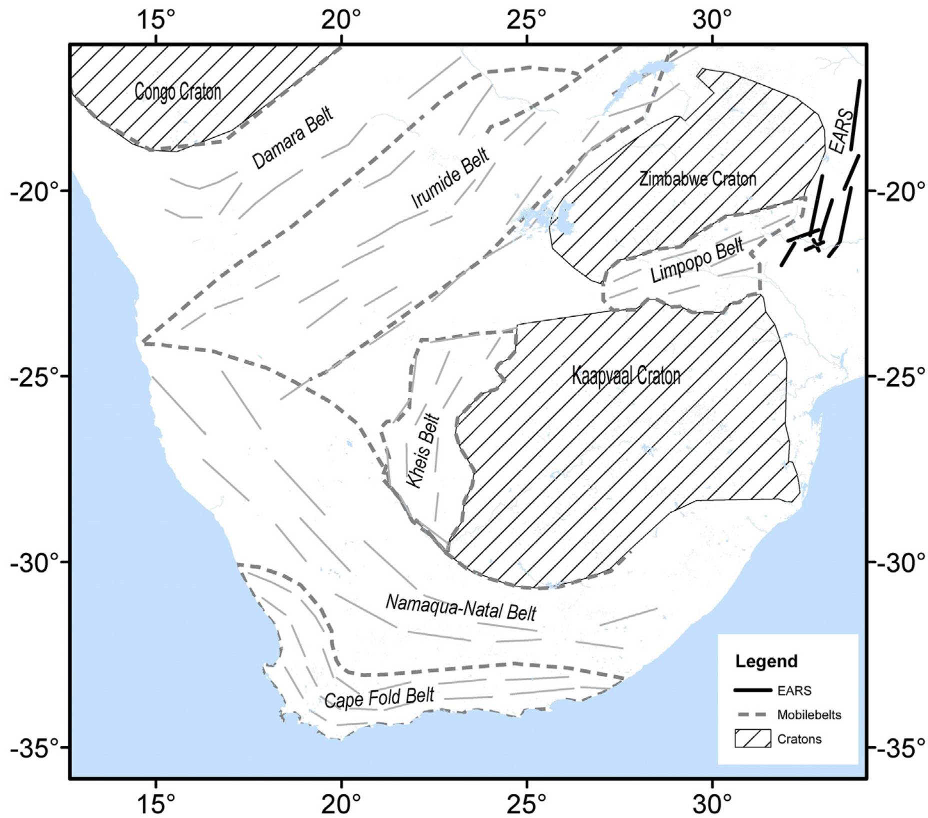

Fig. 2. Basement geology of southern Africa showing the major structural units of the region (from Manzunzu et al., 2019). Broken lines represent uncertain positions of unit boundaries.

was used in the GSHAP seismic hazard assessment for the same region (Midzi et al., 1999). However, it is now almost two decades since this compilation, making it necessary to update and refine the catalogue, especially for southern Africa. Therefore, in this project the earthquake catalogue for South Africa was updated.

The catalogue was prepared by carrying out the following steps:

- Collection of available data mainly from the South African National Seismograph Network (SANSN) including data from the cluster networks around the gold mines in the Witwatersrand Basin (Fig. 2 in Midzi et al., 2015). Other data were obtained from organisations such as the Botswana Geoscience Institute (BGI), the International Seismological Centre (ISC) and Goetz Observatory (1972) in Bulawayo (BUL), Zimbabwe. Valuable data were also obtained from published articles (e.g. Turyomurugyendo, 1996; Mangongolo and Hutchins, 2008).
- The merging of all collected data into one catalogue;
- The removal of duplicate events and mine blasts, with the latter identified by their occurrence at the sites of open cast mines;
- The homogenisation of the earthquake magnitudes to moment magnitude;
- The declustering of the homogenised catalogue.

The compiled catalogue can be divided into the following three subsets to reflect the time varying nature of the information on which the estimation of source parameters and magnitude values is based.

- **Historical data**: This subset includes all events reported that occurred prior to the installation of the first seismograph in South Africa at the Royal Observatory in Cape Town in 1899 (Schweitzer and Lee, 2003; Durrheim, 2015). The assessment of source parameters for this subset is based exclusively on macroseismic data (Fernandez and Guzman, 1979; Brandt et al., 2005; Albini et al., 2014; Strasser et al., 2015).
- **Early instrumental data**: This subset includes all events reported in southern Africa since the turn of the twentieth century after the installation of the first instrument in 1899, until the earthquakes reported just before the 29 September 1969 Ceres/Tulbagh M_W6.2 earthquake. For these events, instrumental recordings mainly confirm the date and time of occurrence, and provide an approximate location based on the distance to the recording instrument(s). A more precise location is generally inferred from macroseismic observations (Albini et al., 2014; Strasser et al., 2015). Similarly, magnitude determinations are only linked to instrumental recordings for larger events occurring during the last two decades of this period. Otherwise they are based on macroseismic observations.
- **Modern instrumental data**: This subset includes all events other than the Ceres sequence (as compiled and reported by Theron, 1974) recorded since the establishment of the SANSN in 1970 (Saunders et al., 2008). Locations and magnitudes for this period are determined from instrumental data, but macroseismic observations are used in some instances to rank and qualify the results.

The specific assumptions made in the determination of source parameters for the above mentioned subsets are detailed in the publications by Fernández and Gúzman (1979), Mangongolo and Hutchins (2008) and Brandt et al. (2005). As would be expected, errors in locations of earthquakes reduced as monitoring of earthquakes improved in the region. A detailed discussion of the accuracy in locations of earthquakes in South African was given in the publication by Saunders et al. (2016). In their study, Brandt et al. (2005) gave a detailed report on how magnitudes of earthquakes in the three subsets discussed above were determined. It was observed that though most of the earthquakes in the catalogue reported local magnitude type (M_L), a few events, reported mainly by the ISC and BUL had body wave magnitude, M_b, values. In cases where only M_b values were reported these were converted to moment magnitude, M_W, using the equations published by Scordillis (2006). In the absence of a published local conversion relation between the M_L values and M_w, the assumption $M_w \approx M_L$ was made. Although empirical relations between M_L and M_w generally show some differences, there is theoretical support for the equivalence between these two magnitude scales (Deichmann, 2006) especially for the moderate size of earthquakes recorded in South Africa. A number of events had published M_w values, which were included in the catalogue as they were (e.g. Strasser et al., 2015; Albini et al., 2014; Brandt and Saunders, 2011; Fan and Wallace, 1995). In their analysis, Bommer et al. (2015) selected a set of global magnitude conversion relations, which they used to convert their data from M_L to M_w. This is the same procedure followed in this study although different relations were used. Bommer et al. (2015) noted the discrepancy in the relations at lower magnitudes, $M_L < 4$, with the global conversion relations. The bulk of the seismicity in South Africa falls below M_L4, hence a relation that takes into account smaller magnitudes was adopted in this study.

Given that the assumption of a Poissonian distribution was made to characterise earthquake occurrences in time, it was necessary to identify and remove dependent events from the catalogue. In this case, dependent events were defined as events whose occurrence is causally linked to that of other events, such as foreshocks and aftershocks, which effectively represent short-term perturbations of the seismicity rate. Prior to the declustering process, human-related events, such as mining-induced events in the mining regions were also removed. The process of identifying and removing such events is tricky. However, it was decided to make an effort to identify them in this study as such events can have a significant effect on the recurrence parameters, thus seismic hazard. The following criteria were used to identify and remove them:

- Location of events in the shallow opencast mining regions (e.g. coal mines)
- Magnitude of events ($M_w \leq 2$) and
- Time of occurrence of events (day time).

Ideally, to satisfy Poissonian distribution, all mining related events should be removed from the catalogue. However, given that moderate to large ($M_w \geq 4.0$) earthquakes have previously occurred in the gold mining regions, it was decided to include these events in the catalogue. Such events have previously caused damage underground and also on the surface. A simplifying assumption was made to treat the sources of induced and/or triggered seismicity as unique seismic sources that are similar to the tectonic sources in that their seismicity will follow a Poisson process. The various mining regions where these events have occurred were therefore included as unique sources in the seismic hazard assessment.

The catalogue was declustered using the cluster-based method by Reasenberg (1985) as applied in the SEISAN software package. It is a simple but reliable technique that has been found not to excessively remove data from the catalogue (Amini, 2014). As a result the technique does not result in the excessive changing of the region activity rate. The algorithm requires the specification of several calibration parameters, time difference, epicentral distance and depth distance. If an event falls into the spatio-temporal window of another, the two events are members of the same cluster. Once all events have been assigned to clusters or found to be independent, the largest event in each cluster is labelled as the mainshock of the cluster, and all events within its spatio-temporal window as dependent events. The latter are then deleted manually to obtain the declustered catalogue. The SEISAN option was selected because it gives the analyst control on the events to be removed from the catalogue. This process resulted in a total of about 10 000 dependent events being removed from the catalogue to leave 50 577 events that can be assumed to be main shocks, ranging from very low magnitude of 0.1 to 7.2. Shown in Fig. 3 are earthquakes obtained from this catalogue for magnitude greater than or equal to 4.0. The main use of the catalogue compiled from the above described process was in the delineation of seismic sources and the estimation of seismicity recurrence parameters to characterise the identified sources.

4. Seismic source characterisation

A seismotectonic model for southern Africa was derived through an analysis of available structural, neotectonic and seismological data to establish links between seismicity and current deformation mechanisms with the ultimate goal being to individualize and delimit the different seismotectonic units (Terrier et al., 2000). Seismotectonic units correspond to individual tectonic structures (e.g., faults) or to geological and structural bodies of uniform seismicity. The idea behind this process is to assist in the identification of potential sources of future earthquakes in South Africa.

However, the identification of actual fault sources of seismicity in the region has proven to be a challenge. This is mainly because earthquakes in the region are generally small to moderate and do not rupture on the surface. In addition, seismicity has been monitored using sparsely distributed seismic stations resulting in large errors in earthquake locations (Saunders et al., 2016). This makes it difficult to clearly associate events with known mapped faults. The high cost of conducting paleoseismic investigations has also made it difficult to investigate the occurrence of earthquakes at specific faults. Exceptions are previous studies carried out along the Kango fault (Fig. 3), which showed that large (approximately magnitude 7.4) earthquakes have occurred along the fault in the past (Goedhart and Booth, 2016a, 2016b). Results from other geological investigations at some of the major faults in the region have also shown them to be active, (e.g., Hebron fault, Dreylingen fault (White et al., 2009), Zebediela and Thabazimbi faults (Good and de Wit, 1997)). In the study to prepare a seismotectonic map of Africa, Meghraoui et al. (2016) identified major faults in southern Africa, some of which were determined to be active by considering available geologic and paleoseismic data, as well as through a rough association of faults with seismicity (Fig. 3).

One major structure on Fig. 3 is the Agulhas fracture zone which stretches in the Indian Ocean parallel to the eastern coast of South Africa. Ben-Avraham et al. (1997) reported that the fracture zone first became active in the Early Cretaceous during the breakup of Gondwana and the passage of the Falkland Island Plateau. However, plate kinematic reconstructions indicate that tectonic activity at the margin ceased approximately 100 Ma (Martin and Hartnady, 1986). Though Ben-Avraham et al. (1995), Parsiegla et al. (2007), and Uenzelmann-Neben and Huhn (2009) all point to possible neotectonic reactivation, no real evidence exists supporting the conclusion that there has been recent tectonic activity along the fracture zone.

The kinematics of faulting and related stress distribution has been the subject of specific studies in the framework of other projects in South Africa (e.g. Fairhead and Girdler, 1971; Shudofsky, 1985; Wagner and Langston, 1988). Focal mechanisms (Fig. 4) and stress field data (Meghraoui et al., 2016) are useful in the characterisation of faults and delineation of seismic source zones. A combination of the few available fault plane solutions, seismicity, basement geology and faults (Fig. 4) is an important tool in the identification of seismic zones.

4.1. Seismic source geometry

The identification of seismic sources is a critical part of seismic hazard analysis and involves a range of data types and scientific interpretations. In his study, Brandt (2008) gave a summary of the types of data usually needed to define each of the four types of seismic sources (i.e. fault, concentrated area zone, regional area zones and background area zones) and the relative usefulness of each data type. However, no requirement is made that all data listed be developed for all hazard analyses as some hazard studies may require more data than others, depending on the scope of the analysis (Budnitz et al., 1997) and availability of relevant data. It is a requirement, however, that all

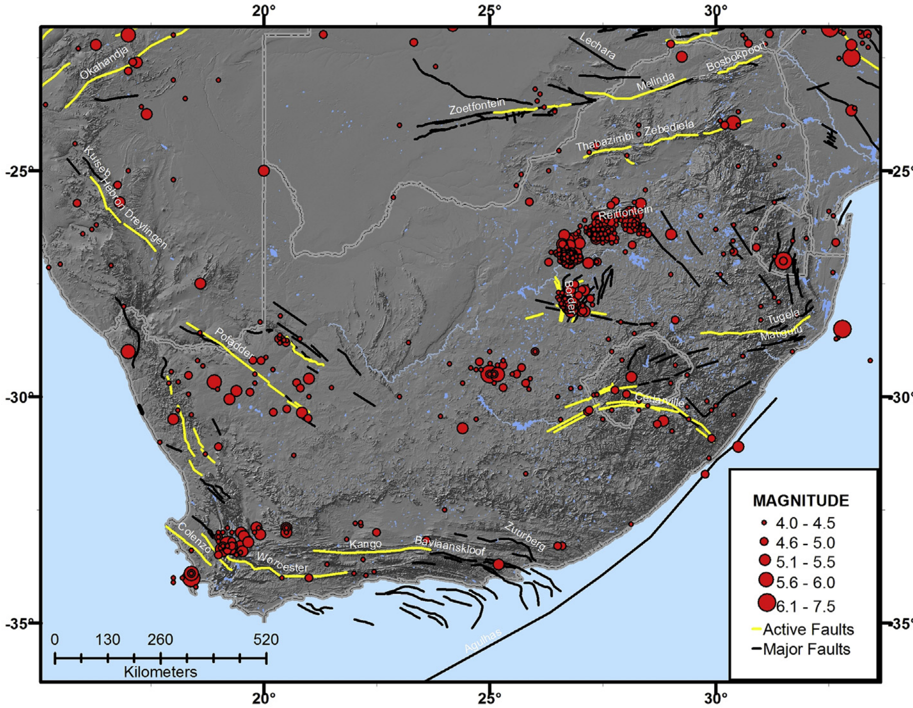

Fig. 3. Major faults of southern Africa, including identified active faults according to the publication by Meghraoui et al. (2016). Also included as red circles are southern African earthquakes of magnitude greater than or equal to 4.0. (For interpretation of the references to colour in this figure legend, the reader is referred to the Web version of this article.)

available data of the type indicated be considered in characterizing the sources. A seismic source model defines the seismogenic potential, location, size, and rate of occurrence of future earthquakes. Ideally the model gives a clear definition of the causative faults that give rise to the observed seismicity. However, information to identify and characterise such faults is limited in South Africa, making the uncertainty associated with characterising the faults too large to confidently use them as unique sources in this study. The alternative, which was adopted in this study, was the creation of a source model made up of characterised area source zones that encompass the possible sources of earthquakes likely to contribute towards the seismic hazard of the region. The available information on faults encompassed in the area sources and focal mechanisms was then used in characterising some of the sources.

The integration and interpretation of the compiled data resulted in the generation of 22 area source zones whose boundaries are shown in Fig. 5. The zones represent areas that can be assumed to be uniform in terms of their seismicity characteristics.

The source zones (Fig. 5) were then delineated as outlined below:

CFBE (Cape Fold Belt East): This zone corresponds to the eastern part of the Cape Fold Belt, which includes a belt of folded Paleozoic sedimentary rock that extends from the south-western margin of the Eastern Cape Province through to the Western Cape Province. Structural trends in the zone are in an east – west direction. The northern boundary is defined by the northern limit of fold and thrust structures, whilst the southern boundary coincides with the continental shelf break and the southern limit of the continental crust. It is bound to the west by the change in direction of structures, which become oriented in a NE to SW direction (Fig. 3). However, the zone exhibits low levels of seismicity, which is in contrast to the higher levels of seismicity in the zone to the west (CFBW). The observed style of faulting

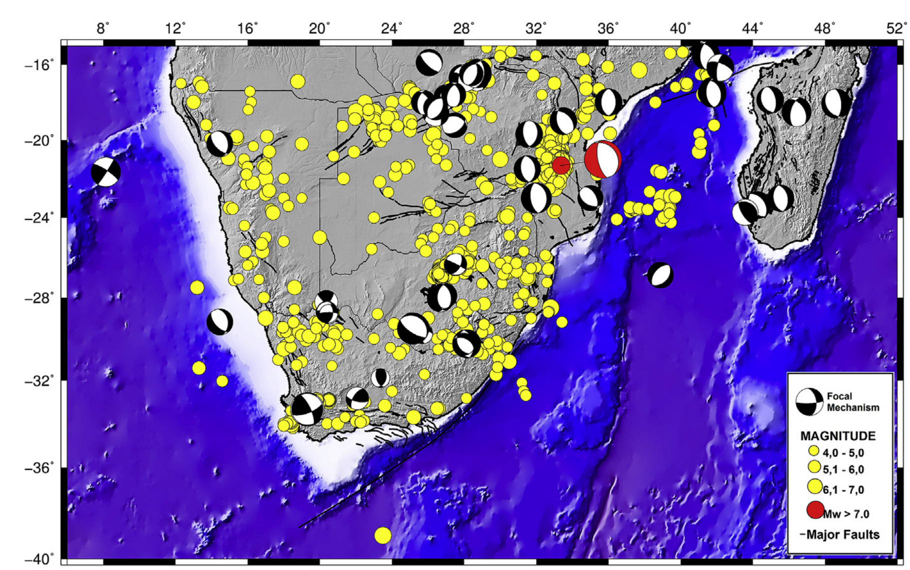

Fig. 4. A seismotectonic map of southern Africa combining available information used in the identification of seismic sources.

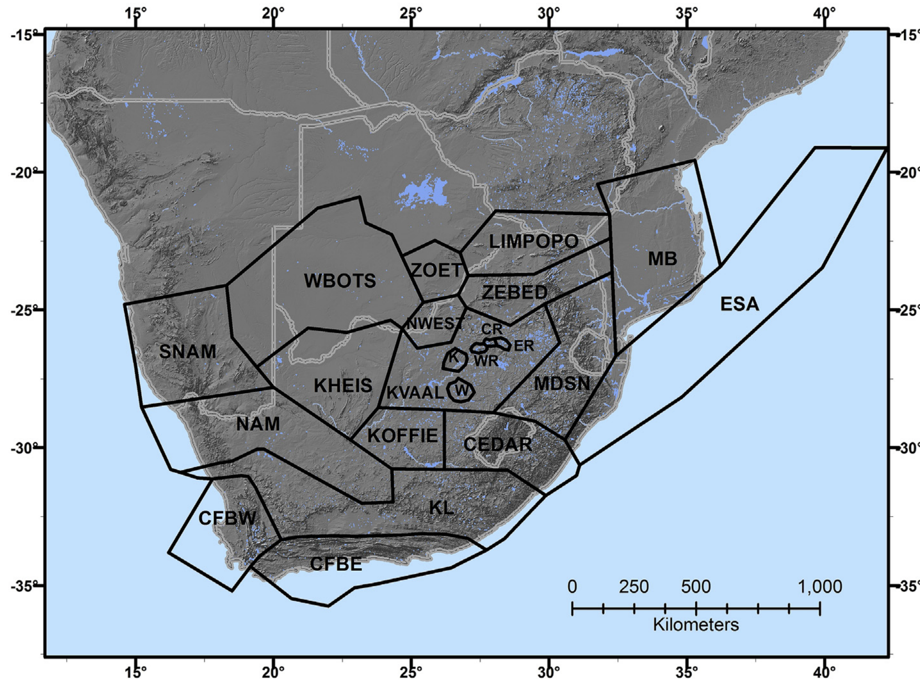

Fig. 5. Illustration of the individual area source zones used in this study. ER- ERAND, WR – WRAND, CR – CRAND, K – KOSH and W – Welkom.

within the CFBE zone (mostly normal faulting) also differs from that assessed for CFBW zone (strike-slip). A recent macroseismic study by Albini et al. (2014) determined source parameters of historical and early instrument earthquakes for which these parameters were not previously available. Paleoseismic investigations conducted along one of the major faults in the zone, the Kango – Baviaanskloof fault (Goedhart and Booth, 2016a, 2016b) confirm the occurrence of large normal faulting earthquakes. The largest recorded earthquake in this zone occurred on 11 September 1969 with a magnitude of M_W5.2. In their interpretation of evidence obtained from results of a paleoseismic investigation along the Kango fault, Bommer et al. (2015), and Goedhart and Booth (2016b), suggest that it is likely that three latest Pleistocene to Holocene surface-faulting events occurred with the largest earthquake having a magnitude of M_w7.2.

CFBW (Cape Fold Belt West): This zone coincides with the syntaxis located at the western end of the Cape Fold Belt. It is characterised by tectonic structures oriented in a NW to SE direction (Fig. 3). Fault plane solutions (e.g. Fig. 4) show strike slip faulting along the faults. The largest observed earthquake in the zone is the M_W6.2, 29 September 1969 Ceres/Tulbagh event, which was felt throughout South Africa. No coseismic surface rupture was documented for this event and thus no particular fault source has been definitively associated with the Ceres earthquake. However, recent studies of seismicity and stress regime of the area (Bird et al., 2006; Krüger and Scherbaum, 2014; Smit et al., 2015) show that the event very likely occurred on one of the active strike-slip NW-SE trending faults in the region.

KL (Karoo Low): The Karoo Low is a seismic zone of sparse and low seismicity where faulting is predominantly normal. The southern boundary is defined by the northern limit of the Cape Fold belt, whilst the northern boundary was modified from the model presented by du Plessis (1996) and coincides with the southern extent of the Namaqua-Natal belt. The maximum observed earthquake in the zone had a magnitude of M_W5.5.

NAM (Namaqualand Zone): This zone coincides with the Namaqua-Natal belt. The stress regime is mainly strike slip in a NNE – SSW and ENE – WSW direction (Johnston et al., 1994). The boundaries were based on those presented by du Plessis (1996) and Singh et al. (2011). Significant earthquakes in the zone include magnitude M_W5.0 events that occurred in 1976 and 1979, as well as the swarm of events observed in the Augrabies area.

KOFFIE (Koffiefontein): The Koffiefontein zone was previously defined by du Plessis (1996) and Singh et al. (2011). It coincides with a cluster of normal faulting events located near Koffiefontein. One of the largest earthquakes in South Africa occurred in this zone in 1912 with a magnitude of M_W6.2, followed by another in 1976 (M_W5.8), both of which were felt widely in southern Africa (Midzi et al., 2013; Strasser et al., 2015).

CEDAR (Cedarville): East of the Koffiefontein zone is the Cedarville zone, which coincides with the active Cedarville fault, as well as a major cluster of events in Lesotho. The zone forms the eastern part of the Namaqua-Natal belt. Though very active, the zone is characterised by events of small to moderate magnitude, with the largest observed earthquake having a magnitude of M_W5.5. Faulting is mainly normal on E-W trending faults.

MDSN (Mpumalanga-Drakensberg-Swaziland-Natal): The MDSN zone is made up of a combination of NE-SW and N-S trending normal faults. The zone is characterised by diffuse seismicity, though a number of moderate events have occurred in the past. The largest observed earthquake occurred on 20 March 1912, with a magnitude of M_W5.0. The zone is bound to the west by the Kaapvaal Craton, the ESA zone to the east, and to the north by the change in orientation of structures to a predominantly ENE-WSW direction (Fig. 3).

KVAAL (Kaapvaal Craton): The zone is approximately bounded by the mobile belts and tectonic structures around the Kaapvaal Craton and is characterised by diffuse background seismicity. Though most of the earthquakes in this zone were small, a few moderately sized events were observed with the largest having a magnitude of M_W4.8. It hosts the mining regions of South Africa and is created to cater for background seismicity outside mining zones. Earthquakes of magnitude less than or equal to 2.0 were removed from the coal mine regions to ensure compliance with Poisson distribution.

LIMPOPO (Limpopo Mobile Belt): This zone is confined within the Limpopo Mobile Belt. The largest observed earthquake had a magnitude of M_W5.0. Structures in the zone generally trend in an ENE-WSW direction. Geological investigations (Holland, 2011) indicate normal faulting along most of the structures, with displacement of aeolian sands along major faults (Bosbokpoort and Melinda faults) and fault scarps ranging from 2 to 10 m in height. In their study, Barker et al. (2006) observed evidence of liquefaction along the Siloam fault, which could have been caused by a large earthquake along the fault.

SNAM (Southern Namibia): The SNAM zone was demarcated mainly using location of observed structures, the major ones of which are the active Hebron and Dreylingen faults (White et al., 2009). It is bound to the south by the Namaqua Mobile Belt which has a higher concentration of seismicity. The northern boundary is the cut off by the Damara Mobile Belt, which has NE-SW trending structures. The eastern boundary is demarcated by the boundary of the Kheis Mobile Belt. The largest earthquake observed in the zone had a magnitude of M_W5.5. Faulting on major structures was observed to be generally normal.

WBOTS (South Western Botswana region): This zone is characterised by some clusters of seismicity, which might be associated with mining activities in the region. The largest observed earthquake in this zone had a magnitude of M_W5.2, which occurred on 8 November 1952. The zone is bound to the south by the northern boundary of the Kheis mobile belt, the Damara belt to the north and western extent of identified major faults in the east.

KHEIS (Kheis Mobile Belt): This zone is entirely located within the Kheis Mobile Belt, whose seismicity is made up mainly of small scattered earthquakes. The largest observed earthquake had a magnitude of M_W3.7. According to Cornell et al. (2011), the Kheis Mobile Belt (Fig. 2) could either be an orogenic belt (~1800 Ma) or a northern branch of the Namaqua-Natal Belt (~1200 Ma). It is described as a thin-skinned region with east-verging thrust belt characteristics. This province is bound by the Kaapvaal Craton to the east.

ESA (Eastern South Africa): This zone encompasses diffuse seismicity, located off the eastern coast of South Africa. A number of moderate to large events have occurred in this area in the past, the largest of which was the magnitude M_W6.3 St Lucia earthquake of December 1932 (Krige and Venter, 1933). Hartnady (1985) proposed a hotspot 'pre-weakening' model arguing that a hotspot moved progressively from Mozambique (ca 60 Ma) through St Lucia (ca 10 Ma) to Cedarville near Lesotho where it is presently located. He also suggested that this might be the point where the East African Rift system (EARS) will extend to in the future.

MB (Mozambique belt): Encompassed in this zone is a region in southern Mozambique where a cluster of seismicity associated with NW-SE oriented faults, including the Machaze fault is located. The largest instrumentally recorded event to occur in southern Africa, the 22 February 2006 Machaze earthquake (M_w7.0), was located in this area. This area is assumed to be part of the southern extension of the EARS and is known to be tectonically more active than other regions in southern Africa. However, inadequate monitoring of earthquakes in Mozambique means that it is difficult to associate observed earthquakes with faults. Only the 2006 Machaze event can be associated clearly with the Machaze fault as surface rupture was observed (Fenton and Bommer, 2006).

ZEBED (Zebediela fault region): The ZEBED source zone is dominated by the NE-SW trending Zebediela and Thabazimbi faults, which appear to be active, but without enough information to be implemented in the study as linear sources. A few moderate earthquakes can clearly be associated with the faults (Fig. 4), with the largest having a magnitude of M_W5.0. In recent investigations (Good and de Wit, 1997; Brandt and Saunders, 2011; Singh et al., 2009, 2011) it was shown that faulting in the region is mainly normal with a strike-slip component, though some reverse faulting was also observed at appropriately oriented branches of the main faults.

ZOET (Zoetfontein fault region): This zone is located in a region located immediately west of the Limpopo Mobile Belt. The main fault in the region is the Zoetfontein fault which has branches mostly trending in a NE-SW and some in a NW-SE direction. The Zoetfontein fault roughly delineates the boundary between the Limpopo Mobile Belt and the Transvaal basins. The eastern part of the fault (Palala Shear Zone) was reactivated at 2 Ga (Dorland et al., 2006), but as shown in Fig. 4, several moderately sized earthquakes can be associated with the fault, implying that it is currently active. According to Jelsma et al. (2009), the fault was reactivated in the late Archean and continues to be active to the present. The recent occurrence of a M_W6.5 earthquake slightly east of the mapped extent of the NW-SE trending branches of the Zoetfontein fault on 3 April 2017 confirms the activity of this fault.

ERAND (East Rand): This is one of the zones in the gold mining regions of South Africa. The ERAND zone has approximately 3400 events, of which 12 have magnitudes greater than or equal to M_W4.0. The largest observed event had a magnitude of M_W4.9. Given the activity observed in this zone, it is possible that earthquakes of magnitude larger than M_W5.0 may occur in the future.

WRAND (West Rand): The WRAND zone is by far the most active of the zones in the mining districts in and around Johannesburg, with a total of about 24 400 events between 1971 and 2014. As with the other two zones (CRAND and ERAND) the events in this zone have remained below M_W5.0 in size, though more than 100 earthquakes of magnitude larger than or equal to M_W4.0 were located in the region, with the largest having a magnitude of M_W4.8.

CRAND (Central Rand): The CRAND source zone, which includes the Johannesburg CBD, has a lower seismicity rate than the East and Western regions. A total of about 1800 events were recorded between 1971 and 2014. The largest event had a magnitude of M_W4.1.

KOSH (Klerksdorp – Orkney – Stilfontein – Hartbeesfontein region): The largest recorded mining-related earthquake in South Africa occurred in the KOSH area on 5 August 2014, with a magnitude of M_W5.5 (Midzi et al., 2015). The event resulted in the death of one person and extensive damage to buildings in the area. A fault plane solution published by Manzunzu et al. (2017) indicates that the event occurred on a strike slip fault, although normal faulting is predominant in this region. The region is quite active with more than 8000 events recorded between 1971 and 2014 as well as about 150 events of magnitude greater than or equal to M_W4.

WELKOM (Welkom gold mining region): This zone is characterised by many earthquakes associated with mining activity. Of the 4143 events in this zone, 39 are of magnitude greater than or equal to M_w4.0. Many of the events appear to be associated with the N-S and NW-SE trending faults observed in the area. Major faults include the Border and de Bron faults. There is evidence of recent fault activation in a trace of 10 km SW of Bultfontein, with a sharp, well defined scarp (Andreoli et al., 1996). Dor et al. (2001) list moderately-sized earthquakes in the Welkom region since 1972. These earthquakes occurred on faults like the Erfdeel, President Brand, and Saaiplaas, with magnitude values ranging between M_W4.7 and M_W5.2. Marshall (1987) undertook a morphotectonic analysis of the Wesselsbron panveld in which convincing evidence was presented for the uplift of a granitic dome to the south-west of Wesselsbron. This, in turn, led to the reactivation of a number of NNW-SSE trending faults (the Eastern Boundary, Border and De Bron faults) located on the eastern flank of the dome. Evidence found underground in mines showed movement along the Dagbreek fault during the 1976 M_W5.1 event.

NWEST (Platinum mines in the North West province): The level of seismicity in the platinum mines is currently low compared to the gold mining region. The observed magnitudes are also currently below M_W5.0 in size.

4.2. Earthquake recurrence parameters

In order to assess the seismic hazard of the region, the identified seismic sources needed to be characterised in terms of their earthquake recurrence, *i.e.* the relative frequency of occurrence of earthquakes with different sizes, as well as the maximum expected earthquake magnitude for each source. The calculations for these parameters were carried out using a maximum-likelihood approach within the ZMAP software (Wiemer, 2001) and SEISAN software (Ottemöller et al., 2013), using

Table 1
Recurrence parameters calculated for source zones considered in the present study. Also included are obtained M_{max} values and earthquake depths and their weights. Techniques used to estimate M_{max} are: TP - Tate-Pisarenko procedure; Norm L1-L1 norm fit of Cumulative Distribution Function of earthquake magnitudes, LS – Classical least squares procedure; K-S – Kijko – Sellevol procedure; N-P-G – Non-parametric with Gaussian kernel procedure, as published by Kijko and Singh (2011). RLD = Subsurface Rupture length in kilometres. M_{max} values in line with RLD values were obtained using a corresponding empirical equation from Wells and Coppersmith (1994). PALEO – refers to values obtained from paleoseismic investigations along the Kango fault (Goedhart and Booth, 2016a, b).

Zone	b value	a value	Weight (b & a pair)	No. of Events	Mobs	Mmax	Mmax Weight	Technique	Depth (km)	Weight
CEDAR	0.93	3.34	0.3	611	5.5	5.85	0.35	TP	5	0.2
	0.85	3.21	0.2			6.04	0.2	Norm L1	10	0.6
	1.06	3.64	0.5			6.36	0.1	LS	15	0.2
						5.73	0.35	K-S		
CFBE	0.7	1.5	0.6	62	5.2	7.2	0.2	PALEO	5	0.2
	1.22	3.63	0.4			6.75	0.4	PALEO	10	0.6
						5.61	0.4	K_S	15	0.2
CFBW	0.9	2.84	0.6	476	6.2	6.74	0.4	TP	5	0.2
	0.77	2.54	0.4			6.62	0.4	K-S	10	0.5
						7.61	0.2	RLD = 132 km	15	0.3
ERAND	1.45	5.47	0.2	3417	4.9	5.11	0.4	N-P-G	2	0.7
	1.48	5.72	0.3			5.4	0.4	TP	5	0.3
	1.27	4.15	0.5			6.3	0.2	RLD = 18.7 km		
CRAND	1.54	5.14	0.2	1820	4.1	5.2	0.65	TP	2	0.7
	1.47	4.9	0.3			5.99	0.35	RLD = 11.8 km	5	0.3
	1.3	4.04	0.5							
KHEIS	1.69	4.4	0.5	1606	3.7	5.28	1.0	TP	2	0.7
	1.73	5.38	0.5						5	0.3
KL	0.78	2.7	0.2	316	5.5	5.73	1.0	TP	5	0.2
	0.88	2.73	0.3						10	0.5
	0.95	3.52	0.5						15	0.3
KOFFIE	0.84	3.01	0.2	247	6	6.43	0.6	TP	5	0.3
	0.78	2.81	0.2			6.00	0.4	LS	10	0.5
	0.97	3.56	0.2						15	0.2
	0.74	2.44	0.4							
KOSH	1.23	5.42	0.5	8736	5.5	5.61	1.0	TP	2	0.6
	1.2	5.39	0.2						5	0.4
	1.04	4.51	0.3							
KVAAL	1.35	4.52	0.3	813	4.8	5.28	0.90	TP	5	0.2
	1.1	3.77	0.6						10	0.6
	1.99	7.41	0.1			6.74	0.10	RLD = 36 km	15	0.2
LIMPOPO	0.62	1.34	0.6	235	5	5.34	1.0	TP	5	0.2
	1.49	4.65	0.4						10	0.6
									15	0.2
ESA	0.79	2.67	0.4	125	6.3	6.76	0.7	K-S	5	0.2
	0.94	3.76	0.3			7.56	0.3	Norm L1	7	0.5
	0.85	3.31	0.3						10	0.3
MB	0.86	4.01	0.34	553	7.2	7.74	0.4	TP	5	0.2
	1.03	4.05	0.33			7.54	0.3	K-S	10	0.6
	0.81	4.68	0.33			7.26	0.3	Norm L1	15	0.2
MDSN	0.79	2.56	0.2	468	5	5.13	0.4	TP	5	0.2
	1.2	4.32	0.3			5.32	0.4	LS	10	0.6
	1.1	3.85	0.5			6.61	0.2	RLD = 30 km	15	0.2
NAM	0.7	2.44	0.2	574	5.8	5.97	1.0	TP	5	0.3
	0.75	2.94	0.3						10	0.5
	0.82	3.61	0.5						15	0.2
NWEST	0.87	1.92	0.6	148	4.6	5.32	1.0	TP	2	0.6
	1.45	3.82	0.4						5	0.4
SNAM	0.8	2.45	0.3	45	5.5	5.96	0.4	TP	5	0.2
	0.96	3.55	0.35			5.8	0.4	K-S	10	0.6
	0.97	3.69	0.35			5.5	0.2	Norm L1	15	0.2
WBOTS	0.81	2.07	0.65	214	5.2	6.11	0.4	K_S	5	0.2
	1.41	4.19	0.35			5.57	0.6	N-P-G	10	0.6
									15	0.2
WELKOM	1.29	5.31	0.4	4143	5.1	5.3	0.7	TP	2	0.6
	1.31	4.79	0.6						5	0.4
						5.6	0.3	M_{obs} + 0.5		
WRAND	1.65	6.93	0.5	24456	4.8	5.2	0.8	TP	2	0.7
	1.52	6.53	0.2			6.34	0.2	RLD = 20 km	5	0.3
	1.32	5.64	0.3							
ZEBED	0.96	2.86	0.6	566	5	5.52	0.45	TP	5	0.2
	1.29	4.25	0.4			5.28	0.45	K-S	10	0.6
						7.23	0.1	RLD = 75.5 km	15	0.2
ZOET	1	2.92	0.6	56	4.4	5.2	0.6	TP	5	0.2
	0.88	2.76	0.4			6.49	0.4	RLD = 25 km	10	0.6
									15	0.2

the declustered catalogue described earlier in Section 3. The seismicity of all sources is assumed to follow a truncated exponential (Gutenberg-Richter) distribution characterised by the following parameters (Gutenberg and Richter, 1944, 1954):

- The M_{max} values, defined as the maximum expected possible earthquake magnitude for each source zone.
- The *b*-value, which represents the slope of the Gutenberg-Richter relation, and controls the relative frequency of occurrence of earthquakes of different magnitudes.
- The activity rate, which is the intercept of the Gutenberg-Richter relation and represents the number of earthquakes with $M_W \geq 0$ occurring each year.

The M_{max} values were estimated mainly through the application of statistical procedures previously published by Kijko and Singh (2011). These techniques make use of the compiled earthquake catalogue for each source zone. For some zones, alternative M_{max} values were estimated using the Wells and Coppersmith (1994) equations that link earthquake magnitude to sub-surface rupture length (Table 1). Faults identified as active in those zones were used in this calculation with the length estimated from segments that can be associated with earthquake locations. Such alternative M_{max} values obtained for each source were used in the hazard calculation in conjunction with assigned weights (W_M) reflecting the level of confidence in each value. These values and weights are summarised in Table 1. In the case of the zone CFBE, the largest magnitude of previous earthquakes identified in the paleoseismic investigation along the Kango fault (Goedhart and Booth, 2016a, b), were used as alternative values of M_{max} for this zone.

4.2.1. Earthquake depth

There is very limited available information on the depth of earthquakes in South Africa. This is mainly because the national seismic network of stations is too sparse to be used to produce reliable depth values (Mangongolo et al., 2017). Limited information is available where advanced analyses such as moment tensor inversion and/or waveform fitting were performed (e.g. Shudofsky, 1985; Jensen, 1991; Dziewonski et al., 1991; Fan and Wallace, 1995; Bowers, 1997; Brandt and Saunders, 2011). However, the studies have clearly shown that earthquakes in South Africa generally occur at shallow depths (Mangongolo et al., 2017; Brandt, 2014; Brandt and Saunders, 2011).

Brandt (2014) determined depth of 24 earthquakes within South Africa. In their analysis tectonic events had depth values ranging from 4 km to 7 km while mining related event depths range from 1 km to 4 km. Given the limited availability of depth information in respect to the distribution of identified source zones, a decision was made to use a set of three alternative values for all of the zones as shown in Table 1. These values cover the range of available depth values and are consistent with typical values observed on continental crust. Lower values were selected for ESA source given that the zone lies entirely in the thinner oceanic crust.

5. Ground motion prediction equations

Ground Motion Prediction Equations (GMPEs) are used to relate a ground-motion parameter (e.g. peak ground acceleration) to a set of variables describing the earthquake source, wave propagation path and local site conditions (e.g. Douglas, 2003). These independent variables invariably include magnitude, source-to-site distance and local site conditions, and often style-of-faulting (mechanism). Some recent models go further to account for other factors affecting earthquake ground motions, such as directivity effects (e.g. Rowshandel, 2006; Spudich et al., 2004; Spudich and Chiou, 2008; Rowshandel, 2010; Shahi and Baker, 2011) and hanging wall effects (e.g. Abrahamson and Silva, 1997; McVerry et al., 2006; Abrahamson and Silva, 2008; Chiou and Youngs, 2014). The GMPE is generally one of the models with the largest influence on the final hazard results. However, it is also generally the largest contributor to uncertainties in hazard.

Given the lack of strong motion data in South Africa, no GMPEs were previously derived specifically for the region. Therefore, two published models from regions of similar tectonics to South Africa were identified as suitable and used in the hazard calculation. Two models were selected in an effort to account for the uncertainty associated with the process of identifying and selecting suitable GMPEs following a procedure similar to that described by Bommer et al. (2010). Both GMPEs were implemented in the hazard calculation by assigning weights to them that represent levels of confidence in the models. Implied in this method is that the selected models represent the composite distribution of epistemic uncertainty in ground motions in this region.

In view of its position relative to plate boundaries, relatively low level of earthquake activity and the slow rates of crustal deformation, South Africa is generally considered a SCR. Therefore, it is considered to be analogous to a region such as the eastern part of North America, for which a number of ground-motion models are available. However, unlike the eastern part of North America, the current tectonic regime of southern Africa shows evidence of extensional tectonic stresses with dominant normal faulting. Bommer et al. (2015) used similar arguments in their seismic hazard study of a site at Thyspunt in South Africa, in deciding against the use of SCR models. Studies such as that by Johnston et al. (1994) show that extensional tectonic stresses are uncommon within SCRs, for which reason the equation of Akkar et al. (2014) is selected as one of the GMPEs used in the seismic hazard assessment. It is an empirical GMPE derived using pan-European datasets for a magnitude range of $4.0 \leq M_W \leq 7.6$ and distance range up 200 km. The GMPE was derived for both point-source (epicentral, R_{EPI} and hypocentral, R_{HYP}) and finite-fault (distance to the surface projection of the rupture, R_{JB}) distance metrics. Akkar et al. (2014) specifically include the V_{s30} value as a predictive parameter within their equation. A clear advantage of the Akkar et al. (2014) GMPE is the ability to explicitly select an appropriate style of faulting.

The model by Boore and Atkinson (2008) also derived for active shallow crustal regions was selected (Table 2) as an alternative GMPE. It also has the advantage of specifically including the average shear-wave velocity over the uppermost 30 m of ground, V_{S30}, as a predictive parameter as well as being able to predict ground motion at long periods. Thus, in this study, it was decided to use the Akkar et al. (2014) GMPE with a higher weight of 0.6 and Boore and Atkinson (2008) a weight of 0.4 for all the sources (Table 2). Both equations were implemented for B/C boundary rock-site conditions (shear-wave velocity of 760 m/s).

In their study Bommer et al. (2015) implemented adjusted versions of two NGA (Next Generation of Attenuation) models (Chiou and Youngs, 2008; Abrahamson and Silva, 2008) as well as the Turkish model of Akkar and Çağnan (2010). The Turkish model was selected to avoid only using NGA models as well as to include a model that is constrained for normal-faulting earthquakes, which dominate in South

Table 2
The two GMPEs selected for use in the PSHA of South Africa.

GMPE	Region	Weight	Remarks
Akkar et al. (2014)	Europe and Middle East	0.6	Active shallow crust. However, mostly events of normal faulting used.
Boore and Atkinson (2008)	Eastern North America	0.4	Active shallow crust. Data used had a mixture of focal mechanisms.

Africa.

6. Seismic hazard calculations

In this study classical probabilistic seismic hazard calculations (Cornell, 1968; McGuire, 1974, 1976; Der Kiureghian and Ang, 1975, 1977) were carried out using the OpenQuake engine, an open source seismic hazard and risk calculation software developed, maintained and distributed by the GEM Foundation (Pagani et al., 2014). A comprehensive manual (Crowley et al., 2015) on the use of the software is available for free on the GEM website and was used extensively in the assessment. The hazard calculations were made for an area consisting of a mesh of 169 sites spaced at approximately 100 km under the following conditions:

- Calculations were made for 10% probability of exceedance in 50 years (or return period of 475 years).
- The minimum magnitude adopted is $M_{min} = 5.0$, which is consistent with the practice of excluding frequent, small events of little engineering significance (EPRI, 1986; Kramer, 1996; Salazar, 2018).
- Calculations were carried out to produce PGA and spectral acceleration maps for one short and a long period, 0.15s and 2.0s respectively.

In cases such as South Africa, where seismic and fault data is limited, uncertainties associated with the input parameters (e.g. recurrence parameters and M_{max} values) need to be assessed and considered in the hazard calculations. In this study, alternative values of input parameters were obtained and implemented in the hazard calculation using a logic tree technique (e.g. logic tree for KVAAL source in Fig. 6 and input parameters in Table 1). These logic trees provide a convenient form for the formal and quantitative treatment of the uncertainties and have been used this way for a while in probabilistic seismic hazard assessments (e.g. Kulkarni et al., 1984; Coppersmith and Youngs, 1986; Reiter, 1990).

7. Results and discussion

Mean seismic hazard maps for a return period of 475 years (10% probability of exceedance in 50 years) of three ordinates (PGA, 0.15s and 2.0s) were produced (Figs. 7–9 respectively).

The highest seismic hazard values are observed in the KOSH gold mining region of South Africa. However, at long period (2.0s) the highest hazard is observed in the north-eastern part of the country which is likely an influence of the MB source which has a record of large earthquakes. The high acceleration observed in the KOSH region at lower periods could be a result of the shallow moderate earthquakes in that area as well as the high activity rates associated with the mining related earthquakes. Results of sensitivity analyses (Midzi et al., 2016) showed that the hazard in that area is certainly driven by the recurrence parameters. Interestingly, the hazard in the south-western part of South Africa where the largest recorded earthquake in South Africa (M_w6.2)

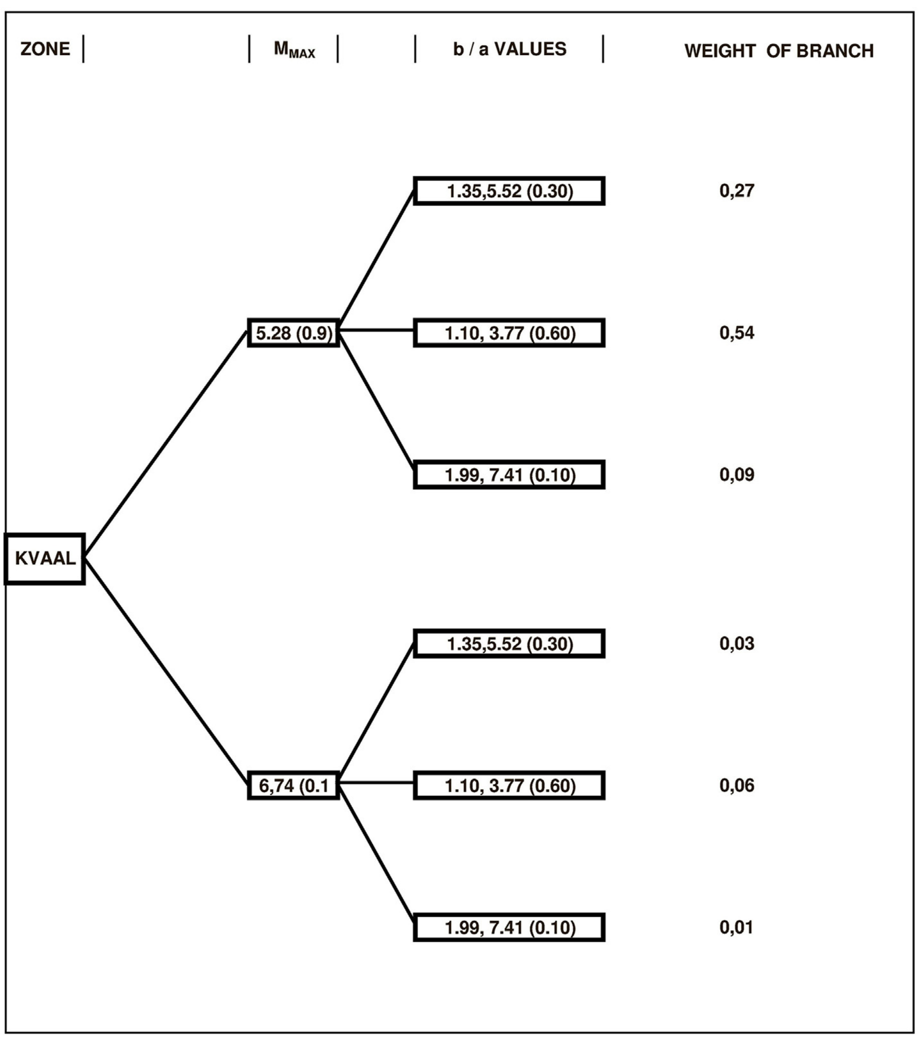

Fig. 6. Typical seismic source characterisation logic tree for the area sources zones determined in this study (e.g. given here is the logic tree for KVAAL source zone).

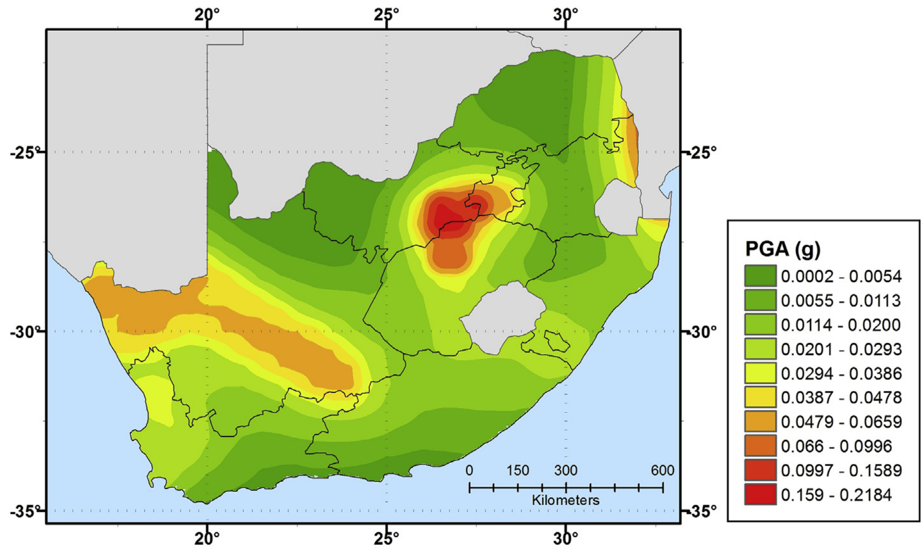

Fig. 7. Distribution of mean PGA values in South Africa computed for 10% probability of exceedance in 50 years (return period of 475 years).

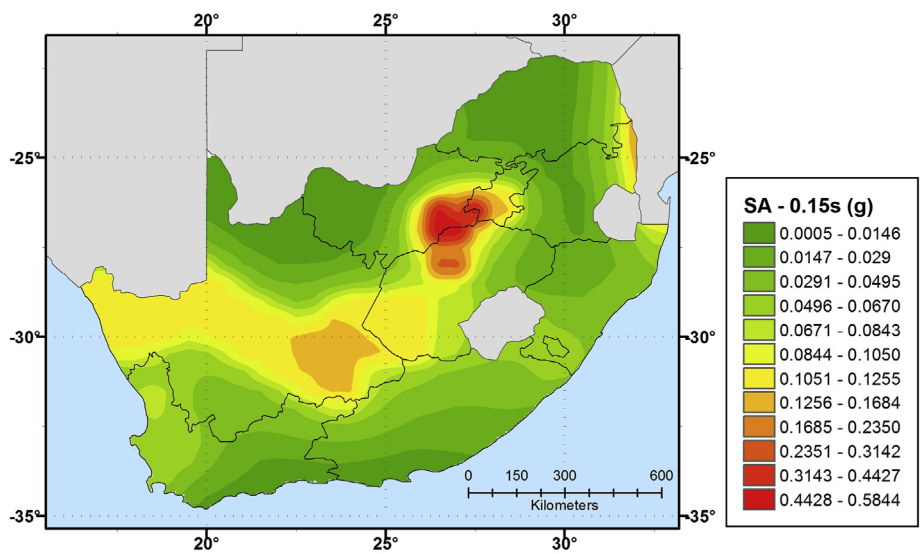

Fig. 8. Distribution of spectral acceleration (period of 0.15s) values in South Africa computed for 10% probability of exceedance in 50 years (return period of 475 years).

occurred on 29 September 1969 is relatively low for all three maps (Figs. 7–9). This is observed to be due to the low activity rates observed in the area as illustrated by the low 'a-value' for zone CFBW especially when compared to other zones (Table 1).

On comparing the results obtained in this study to those from previous studies (e.g. Fernández and du Plessis, 1992; Midzi et al., 1999; Kijko et al., 2003), it was found that the PGA values in the Witwatersrand gold mining region were similar in magnitude with maximum values of about 0.2 g (Fig. 7). However, the distribution of the values is not similar. Previous maps (e.g. Fernández and du Plessis, 1992; Kijko et al., 2003) have other areas of PGA values of 0.2 g such as the Ceres and the Koffiefontein areas. These areas have previously experienced large earthquakes. It appears the results by Fernández and du Plessis (1992) and Kijko et al. (2003) are driven by the distribution of clusters of seismicity especially where large events occurred in the past. This is not surprising given that their methodology does not consider seismic zones but earthquake distribution. The results obtained by Midzi et al. (1999), have lower acceleration values but with areas of their values coincident with the location of source zones used in their calculation. PGA values of less than 0.02 g were observed in the Witwatersrand basin, mainly because in their study, Midzi et al. (1999) did not include areas with mining-related earthquakes in their seismic source model in order to meet the Poisson distribution condition.

8. Conclusion

The results obtained in the present study provide the first hazard maps for South Africa prepared using a probabilistic seismic hazard assessment approach where seismic source zones are used. An effort was made to include geological information in addition to available seismic data, fault plane solutions and stress regime data. A combination of these data together with previously published information on the seismotectonics of the region (e.g. Hartnady, 1985; du Plessis, 1996; Andreoli et al., 1996; Singh et al., 2011; Brandt and Saunders, 2011), produced a well-constrained seismic source model. Uncertainties associated with inadequate data (e.g. incomplete and short earthquake catalogue, limited information on earthquake depth values) were addressed in the calculation by considering alternative values of the input

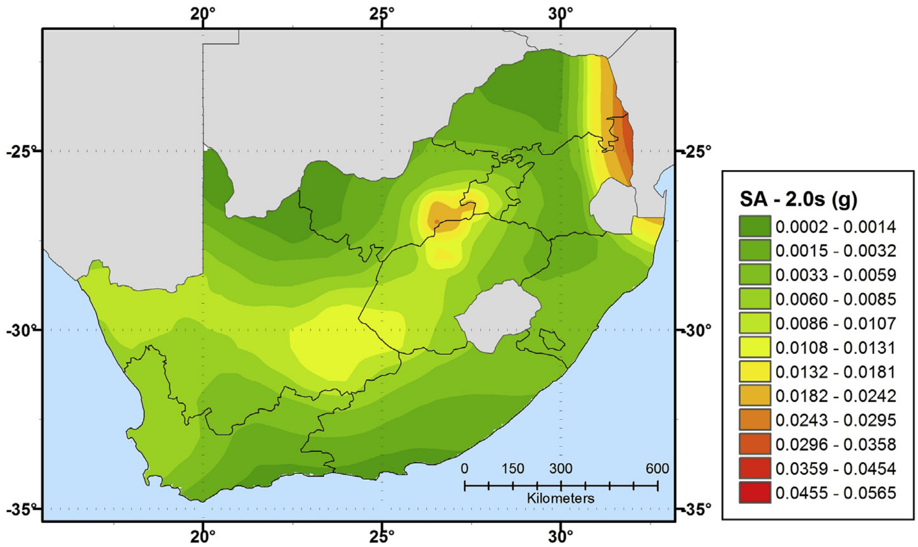

Fig. 9. Distribution of spectral acceleration (period of 2.0s) values in South Africa computed for 10% probability of exceedance in 50 years (return period of 475 years).

parameters, which were then implemented through the use of the logic tree technique. However, a major weakness of the study is the unavailability of a GMPE designed specifically for South African conditions. Ideally, it is necessary to have equations for the different sources of earthquakes in South Africa, induced events (mining related) and natural events (tectonic), as well as the different tectonic regimes (cratons and mobile belts). However, this lack of suitable GMPEs was addressed by adopting equations derived for tectonically similar regions especially with similar style of faulting. Two equations (Akkar et al., 2014; Boore and Atkinson, 2008) were selected and implemented in the calculation with assigned weights, again using the logic tree technique.

Ground acceleration distribution is driven mainly by the delineated seismic source zones, with the KOSH zone contributing much of the hazard at all periods considered. Other mining region sources (i.e. WRAND and WELKOM) also contributed much hazard though more on a local scale unlike KOSH. The impact of large earthquakes in the MB zone is felt mainly in the north-eastern part of the country especially at longer periods.

A major assumption made in this study is that the seismicity associated with mining regions is stationary with its temporal and spatial distribution following a Poissonian distribution. However, this is not necessarily true as the events appear to depend on human activity. In future, this temporal variation and spatial distribution will need to be assessed and its effect incorporated in the computation.

As much as the results of this study form a valuable addition to available information on the seismic hazard of South Africa, it is strongly recommended that these results should not be used directly for design purposes of structures but rather for planning purposes. However, the information included here can be used in conducting a site specific probabilistic seismic hazard assessment for the particular structures to be constructed at the site.

Funding

The research did not receive any specific grant from funding agencies in the public, commercial, or not-for-profit sectors. However, the Council for Geoscience of South Africa funded the work from internal research funds.

Acknowledgements

The authors are grateful for the assistance and information contributed by the IGCP601 project (Seismotectonic Map of Africa). Their contribution was very useful in the preparation of the seismic source model. The Global Earthquake Model's (GEM) assistance in providing free the OPENQUAKE software and technical assistance whenever needed is also much appreciated.

Appendix A. Supplementary data

Supplementary data to this article can be found online at https://doi.org/10.1016/j.jafrearsci.2019.103689.

References

Abrahamson, N.A., Silva, W.J., 1997. Empirical response spectral attenuation relations for shallow crustal earthquakes. Seismol. Res. Lett. 68 (1), 94–127.

Abrahamson, N.A., Silva, W.J., 2008. Summary of the Abrahamson & Silva NGA ground-motion relations. Earthq. Spectra 24 (1), 67–97.

Adams, A., Nyblade, A., 2011. Shear wave velocity structure of the southern African upper mantle with implications for the uplift of southern Africa. Geophys. J. Int. 186, 808–824.

Albini, P., Strasser, F.O., Flint, N.S., 2014. Earthquakes from 1820 to 1936 in Grahamstown and surroundings (eastern Cape province, South Africa). Bull. Earthq. Eng. 12 (1), 45–78.

Amini, H., 2014. Comparing Reasenberg and Gruenthal declustering methods for north of Iran. In: 2nd European Conference on Earthquake Engineering and Seismology, pp. 7.

Andreoli, M.A.G., Doucouré, M., van Bever Donker, J., Brandt, D., Andersen, N.J.B., 1996. Neotectonics of southern Africa – a review. Afr. Geosci. Rev. 3 (1), 1–16.

Akkar, S., Çağnan, Z., 2010. A local ground-motion predictive model for Turkey and its comparison with other regional and global ground-motion models. Bull. Seismol. Soc. Am. 100 (6), 2978–2995.

Akkar, S., Sandıkkaya, M.A., Ay, B.Ö., 2014. Empirical ground-motion models for point- and extended-source crustal earthquake scenarios in Europe and the Middle East. Bull. Earthq. Eng. 12 (1), 359–387.

Barker, O.B., Brandl, G., Callaghan, C.C., Weiksson, P.G., Van der Neut, M., 2006. The Soutpansberg and Waterberg Groups and the Blouberg formation. In: Johnson, M.R., Anhaeusser, C.R., Thomas, R.J. (Eds.), The Geology of South Africa, Geological Society of South Africa. Johannesburg/Council for Geoscience, Pretoria, South Africa, pp. 301–318.

Ben-Avraham, Z., Hartnady, C.J.H., le Roux, A.P., 1995. Neotectonic activity on continental fragments in the southwest Indian Ocean: Agulhas Plateau and Mozambique ridge. J. Geophys. Res. 100 (B4), 6199–6211.

Ben-Avraham, Z., Hartnady, C.J.H., Kitchin, K.A., 1997. Structure and tectonics of the Agulhas-Falkland fracture zone. Tectonophysics 282 (1), 83–98.

Bird, P., Ben-Avraham, Z., Schubert, G., Andreoli, M.A.G., Viola, G., 2006. Patterns of stress and strain rate in South Africa. J. Geophys. Res. 111, B08402. https://doi.org/10.1029/2005JB003882.

Bommer, J.J., Coppersmith, K.J., Coppersmith, R.T., Hanson, K.T., Mangongolo, A., Neveling, J., Rathje, E.M., Rodriguez-Marek, A., Scherbaum, F., Shelembe, R., Stafford, P.J., Strasser, F.O., 2015. A SSHAC Level 3 Probabilistic Seismic Hazard Analysis for a New-Build Nuclear Site in South Africa. Earthquake Spectra 31 (2), 661–698. https://doi.org/10.1193/060913EQS145M.

Bommer, J.J., Douglas, J., Scherbaum, F., Cotton, F., Bungum, H., Fäh, D., 2010. On selection of ground-motion prediction equations for seismic hazard analysis. Seismol. Res. Lett. 81 (5), 783–793.

Boore, D.M., Atkinson, G.M., 2008. Ground-motion prediction equations for the average horizontal component of PGA, PGV, and 5%-damped PSA at spectral periods between 0.01 s and 10.0 s. Earthq. Spectra 24 (1), 99–138.

Booth, P.W.K., Brunsdon, G., Shone, R.W., 2004. A duplex model for the eastern Cape Fold belt? Evidence from the Palaeozoic Witteberg and Bokkeveld Groups (Cape Supergroup), near Steytlerville, South Africa. Gondwana Res. 7, 211–222.

Bowers, D., 1997. The October 30, 1994, seismic disturbance in South Africa: earthquake or large rock burst? J. Geophys. Res. 102 (B5), 9843–9857.

Brandt, M.B.C., 2008. Review of the Seismotectonic Provinces and Major Structures in South Africa with New Data. Council for Geoscience Report Number 2008-0001.

Brandt, M.B.C., Saunders, I., 2011. New regional moment tensors in South Africa. Seismol. Res. Lett. 82 (1), 69–80.

Brandt, M.B.C., Bejaichund, M., Kgaswane, E.M., Hattingh, E., Roblin, D.L.R., 2005. Seismic History of Southern Africa, vol. 37 Council for Geoscience Seismological Series.

Brandt, M.B.C., 2014. Focal depths of South African earthquakes and mine events. J. S. Afr. Inst. Min. Metall 114, 1–8.

Budnitz, R.J., Apostolakis, G., Boore, D.M., Cluff, L.S., Coppersmith, K.J., Cornell, C.A., Morris, P.A., 1997. Recommendations for Probabilistic Seismic Hazard Analysis: Guidance on Uncertainty and Use of Experts. Appendices NUREG/CR-6372 2.

Chiou, B.J., Youngs, R.R., 2008. An NGA model for the average horizontal component of peak ground motion and response spectra. Earthq. Spectra 24, 173–215.

Chiou, B.J., Youngs, R.R., 2014. Update of the Chiou and Youngs NGA model for the average horizontal component of peak ground motion and response spectra. Earthq. Spectra 30 (3), 1117–1153.

Coppersmith, K.J., Youngs, R.R., 1986. Capturing uncertainty in probabilistic seismic hazard assessments within intraplate tectonic environments. In: Proceedings of the Third U.S. National Conference on Earthquake Engineering. vol. 1. pp. 301–312.

Cornell, C.A., 1968. Engineering seismic risk analysis. Bull. Seismol. Soc. Am. 18, 1583–1606.

Cornell, D.H., van Schijndel, V., Ingolfsson, O., Scherstén, A., Karlsson, L., Wojtyla, J., Karlsson, K., 2011. Evidence from Dwyka tillite cobbles of Archaean basement beneath the Kalahari sands of southern Africa. Lithos 125, 482–502.

Crowley, H., Monelli, D., Pagani, M., Silva, V., Weatherill, G., Rao, A., 2015. The OpenQuake-Engine User Manual. Global Earthquake Model (GEM) Technical Report 2015-09. https://doi.org/10.13117/GEM. OPENQUAKE.MAN.ENGINE.1.5/01.

de Wit, M.J., Ransome, I.G.D., 1992. Regional inversion tectonics along the southern margin of Gondwana. In: de Wit, M.J., Ransome, I.G.D. (Eds.), Inversion Tectonics of the Cape Fold Belt, Karoo and Cretaceous Basins of Southern Africa. Balkema AA, Rotterdam, pp. 15–21.

Deichmann, N., 2006. Local magnitude, a moment revisited. Bull. Seismol. Soc. Am. 96 (4A), 1267–1277.

Der Kiureghian, A., Ang, A.H.S., 1975. A Line Source Model for Seismic Risk Analysis. University of Illinois Technological Report, pp. 134 UILU-ENG-75-2023.

Der Kiureghian, A., Ang, A.H.S., 1977. A fault-rupture model for seismic risk analysis. Bull. Seismol. Soc. Am. 67, 1173–1194.

Dor, O., Reches, Z., van Aswegen, G., 2001. Fault Zones Associated with Matjhabeng Earthquake, 1999, South Africa. Rockbursts and Seismicity in Mines – RaSiM5. South African Institute of Mining and Metallurgy.

Dorland, H.C., Beukes, N.J., Gutzmer, J., Evans, D.A.D., Armstrong, R.A., 2006. Precise SHRIMP U-Pb zircon age constraints on the lower Waterberg and Soutpansberg Groups, South Africa. S. Afr. J. Geol. 109, 139–156.

Douglas, J., 2003. Earthquake ground motion estimation using strong-motion records: a review of equations for the estimation of peak ground acceleration and response spectral ordinates. Earth Sci. Rev. 61 (1–2), 43–104.

Du Plessis, A., 1996. Seismicity in South Africa and its Relationship to the Geology of the Region. Council for Geoscience Report No. 1996-0019.

Durrheim, R.J., 2015. Earthquake Seismology. In: de Beer, J.H. (Ed.), History of Geophysics in Southern Africa, South Africa Geophysical Association.

Dziewonski, A.M., Ekström, G., Woodhouse, J.H., Zwart, G., 1991. Centroid-moment tensor solutions for July–September 1990. Phys. Earth Planet. Inter. 67, 211–220.

EPRI, 1986. Methodology. Seismic Hazard Methodology for the Central and Eastern United States, vol. 1 Electric Power Research Institute, Palo Alto, California Rept. EPRI NP-4726.

Fairhead, J.D., Girdler, R.W., 1971. The seismicity of Africa. Geophys. J. 24 (3), 271–301.

Fan, G., Wallace, T., 1995. Focal mechanism of a recent event in South Africa: a study using a sparse very broadband network. Seismol. Res. Lett. 66 (5), 13–18.

Fenton, C.H., Bommer, J.J., 2006. The Mw7 Machaze, Mozambique, earthquake of 23 February 2006. Seismol. Res. Lett. 77 (4), 426–439.

Fernández, L.M., du Plessis, A., 1992. Seismic Hazard Maps of Southern Africa. Geological Survey of South Africa, Pretoria, South Africa.

Fernandez, L.M., Guzman, J.A., 1979. Seismic history of southern Africa. Geological Survey of South Africa Seismologic Series 9, 1–38.

Field, E.H., Jordan, T.H., Cornell, C.A., 2003. OpenSHA—a developing community-modeling environment for seismic hazard analysis. Seismol. Res. Lett. 74, 406–419.

Gane, P.G., 1939. A statistical study of the Witwatersrand earth tremors. J. Chem. Metall. Min. Soc. S. Afr. 40, 155–172.

Gane, P.G., Oliver, H.O., 1953. South Arican earthquakes - 1949 to December, 1952. Trans. Geol. Soc. S. Afr. 56, 21–33.

Giardini, D., Grünthal, G., Shedlock, K.M., Zhang, P.Z., 1999. The GSHAP global seismic hazard map. Ann. Geofisc. 42 (6), 1225–1230.

Goedhart, M.L., Booth, P.W.K., 2016a. A palaeoseismic trench investigation of early Holocene neotectonic faulting along the Kango Fault, southern Cape Fold Belt, South Africa–Part I: stratigraphic and structural features. S. Afr. J. Geol. 119, 545–568.

Goedhart, M.L., Booth, P.W.K., 2016b. A palaeoseismic trench investigation of early Holocene neotectonic faulting along the Kango Fault, southern Cape Fold Belt, South Africa–Part II: earthquake parameters. S. Afr. J. Geol. 119, 569–582.

Goetz Observatory, 1972. A Seismological Study of Earthquakes in the Southwest Cape Province 1969-1970. Goetz Observatory Technical Report. Meteorological Department, Bulawayo.

Good, N., de Wit, M.J., 1997. The Thabazimbi-Murchinson lineament of the Kaapvaal craton, South Africa: 2700 Ma of episodic deformation. J. Geol. Soc. 154, 93–97.

Gutenberg, B., Richter, C.F., 1944. Frequency of earthquakes in California. Bull. Seismol. Soc. Am. 34 (4), 185–188.

Gutenberg, B., Richter, C.F., 1954. Seismicity of the Earth. Princeton Press.

Hälbich, I.W., 1983. A geodynamic model for the Cape Fold belt (CFB). In: Sönghe, A.P.G., Hälbich, I.W. (Eds.), Geodynamics of the Cape Fold Belt: A Contribution to the National Geodynamics Programme, Special Publication 12. Geological Society of South Africa, Johannesburg, pp. 177–184.

Hartnady, C.J.H., 1985. Uplift, faulting, seismicity, thermal spring and possible incipient volcanic activity in the Lesotho-Natal region, SE Africa: the Quathamba hotspot hypothesis. Tectonics 4, 371–377.

Holland, M., 2011. Hydrogeological Characterisation of Crystalline Basement Aquifers within the Limpopo Province, South Africa. PhD Thesis. University of Pretoria, South Africa.

International Federation of Red Cross and Red Crescent Societies, 2010. World Disasters Report. 978-92-9139-156-1.

Jelsma, H., Barnett, W., Richards, S., Lister, G., 2009. Tectonic setting of kimberlites. Lithos 112S, 155–165.

Jensen, B.L., 1991. Source Parameters and Seismotectonics of Three Earthquakes in the Stable Continental Interior of Africa. MSc Thesis. Memphis State University.

Johnston, A.C., Coppersmith, K.J., Kanter, L.R., Cornell, C.A., 1994. The Earthquakes of Stable Continental Regions. Electric Power Research Institute Report (EPRI), Palo Alto, CA.

Kijko, A., Graham, G., 1998. Parametric-historic procedure for probabilistic seismic hazard analysis Part I: estimation of maximum regional magnitude m_{max}. Pure Appl. Geophys. 152, 413–442.

Kijko, A., Graham, G., 1999. Parametric-historic procedure for probabilistic seismic hazard analysis Part II: assessment of seismic hazard at specified site. Pure Appl. Geophys. 154, 1–22.

Kijko, A., Singh, M., 2011. Statistical tools for maximum possible earthquake magnitude estimation. Acta Geophys. 59 (4), 674–700.

Kijko, A., Graham, G., Bejaichund, M., Roblin, D., Brandt, M.B.C., 2003. Probabilistic Peak Ground Acceleration and Spectral Seismic Hazard Maps for South Africa. Council for Geoscience, Pretoria Report Number 2003-0053.

Kramer, S.L., 1996. Geotechnical earthquake engineering. In: Prentice–Hall International Series in Civil Engineering and Engineering Mechanics. Prentice-Hall, New Jersey.

Krige, L.J., Venter, F.A., 1933. The Zululand earthquake of the 31st December 1932. Trans. Geol. Soc. S. Afr. 36, 101–112.

Krüger, F., Scherbaum, F., 2014. The 29 September 1969, Ceres, South Africa, earthquake: Full waveform moment tensor inversion for point source and kinematic source parameters. Bull. Seismol. Soc. Am. 104, 576–581.

Kulkarni, R.B., Youngs, R.R., Coppersmith, K.J., 1984. Assessment of confidence intervals for results of seismic hazard analysis. In: Proceedings of the Eighth World Conference on Earthquake Engineering. vol. 1. pp. 263–270 San Francisco.

Malephane, H., 2007. Seismicity and Seismic Hazard of Lesotho. MSc thesis. University of Bergen, Bergen, Norway.

Mangongolo, A., Hutchins, D.G., 2008. Seismicity of Namibia from 1910 to 2006. In: Miller, R. (Ed.), Geology of Namibia. Geological Survey of Namibia, Windhoek.

Mangongolo, A., Strasser, F.O., Saunders, I., Rathod, G.W., 2017. Depths of earthquakes in South Africa. Seismol. Res. Lett. 88 (4), 1078–1088.

Manzunzu, B., Midzi, V., Mangongolo, A., Essrich, F., 2017. The aftershock sequence of the 5 August 2014 Orkney earthquake (ML 5.5), South Africa. J. Seismol. 21 (6), 1323–1334.

Manzunzu, B., Midzi, V., Mulabisana, T.F., Zulu, B., Pule, T., Myendeki, S., Rathod, G.W., 2019. Seismotectonics of South Africa. J. Afr. Earth Sci. 149, 271–279.

Marshall, T.R., 1987. Morphotectonic analysis of the Wesselsbron panveld. S. Afr. J. Geol. 90, 209–218.

Martin, A.K., Hartnady, C.J.H., 1986. Plate tectonic development of the south west Indian ocean: a revised reconstruction of East Antarctica and Africa. J. Geophys. Res. 91 (B5), 4767–4786.

McGuire, R.K., 1974. Seismic Structural Response Risk Analysis, Incorporating Peak Response Regressions on Earthquake Magnitude and Distance. Massachussets Technical. Department of Civil Engineering, Publication No. 399, pp. 371.

McGuire, R.K., 1976. FORTRAN computer program for seismic risk analysis. U.S Geological Survey Open-File Report 76–67, 90.

McGuire, R.K., 2004. Seismic Hazard and Risk Analysis. Earthquake Engineering Research Institute, Oakland.

McVerry, G.H., Zhao, J.X., Abrahamson, N.A., Somerville, P.G., 2006. New Zealand acceleration response spectrum attenuation relations for crustal and subduction zone earthquakes. Bull. N. Z. Soc. Earthq. Eng. 39 (4), 1–58.

Meghraoui, M., Amponsah, P., Ayadi, A., Ayele, A., Ateba, B., Bensuleman, A., Delvaux, D., El Gabry, M., Fernandes, R., Midzi, V., Roos, M., Timoulali, Y., 2016. The seismotectonic map of Africa. Episodes 39 (1), 9–18.

Midzi, V., Hlatywayo, D.J., Chapola, L.S., Kebede, F., Atakan, K., Lombe, D.K.,

Turyomurugyendo, G., Tugume, F.A., 1999. Seismic hazard assessment in eastern and southern Africa. Ann. Geofisc. 42 (6), 1067–1083.
Midzi, V., Bommer, J.J., Strasser, F.O., Albini, P., Zulu, B.S., Prasad, K., Flint, N.S., 2013. An intensity database for earthquakes in South Africa from 1912 to 2011. J. Seismol. 17, 1183–1205.
Midzi, V., Zulu, B., Manzunzu, B., Mulabisana, T., Pule, T., Myendeki, S., Gubela, W., 2015. Macroseismic survey of the ML5.5, 2014 Orkney earthquake. J. Seismol. 19 (3), 741–751.
Midzi, V., Manzunzu, B., Mulabisana, T., Zulu, B.S., Pule, T., Myendeki, S., Rathod, G.W., 2016. The Probabilistic Seismic Hazard Assessment of South Africa. Council for Geoscience Report No. 2016-0064.
Oman, S.D., Manor, O., Shishinski, R., Shapira, A., 1984. Seismic Hazard Estimations Program - a Preliminary Report Z6. The Institute for Petroleum Research and Geophysics, Holon, Israel, Republic, pp. 35 3.
Ottemöller, L., Voss, P., Havskov, J., 2013. Seisan earthquake analysis software for WINDOWS, SOLARIS, LINUX and MACOSX. http://seis.geus.net/software/seisan/seisan.pdf, Accessed date: 12 March 2013.
Pagani, M., Monelli, D., Weatherill, G., Danciu, L., Crowley, H., Silva, V., Henshaw, P., Butler, L., Nastasi, M., Panzeri, L., Simionato, M., Vigano, D., 2014. OpenQuake-engine: an open hazard (and risk) software for the global earthquake model. Seismol. Res. Lett. 85, 692–702.
Parsiegla, N., Gohl, K., Uenzelmann-Neben, G., 2007. Deep crustal structure of the sheared South African continental margin: first results of the Agulhas-Karoo Geoscience Transect. S. Afr. J. Geol. 110, 393–406.
Pule, T., Fourie, C.J.S., Kijko, A., Midzi, V., 2015. Comparison and quantitative study of vulnerability/damage curves in South Africa. S. Afr. J. Geol. 118 (4), 335–354.
Reasenberg, P., 1985. Second-order moment of central California seismicity, 1969 – 1982. J. Geophys. Res. 90, 5479–5495.
Reiter, L., 1990. Earthquake Hazard Analysis: Issues and Insight. Columbia University Press, New York.
Rowshandel, B., 2006. Incorporating source rupture characteristics into ground-motion hazard analysis models. Seismol. Res. Lett. 77 (6), 708–722.
Rowshandel, B., 2010. Directivity correction for the Next generation attenuation (NGA) relations. Earthq. Spectra 26 (2), 525–559.
Salazar, W., 2018. Principles of probabilistic seismic hazard assessment (PSHA) and site effect evaluation and its application for the volcanic environment in El Salvador. In: Svalova, V. (Ed.), Earthquakes: Forecast, Prognosis and Earthquake Resistant Construction, https://doi.org/10.5772/intechopen.75845.
Saunders, I., Brandt, M.B.C., Steyn, J., Roblin, D., Kijko, A., 2008. The South African national seismograph network. Seismol. Res. Lett. 79, 203–210.
Saunders, I., Kijko, A., Fourie, C.J.S., 2016. Statistical evaluation of seismic event location accuracy by the South African National Seismograph Network over four decades. S. Afr. J. Geol. 119 (1), 291–304.
Schweitzer, J., Lee, W.H.K., 2003. Old seismic bulletins to 1920: a collective heritage from early seismologists. In: Lee, W., Jennings, P., Kisslinger, C., Kanamori, H. (Eds.), International Handbook of Earthquake & Engineering Seismology, Part B. Academic Press, pp. 1665–1723.
Scordilis, E.M., 2006. Empirical global relations converting MS and mb to moment magnitude. J. Seismol. 10, 225–236.
Shahi, S.K., Baker, J.W., 2011. An empirically calibrated framework for including the effects of near-fault directivity in probabilistic seismic hazard analysis. Bull. Seismol. Soc. Am. 101 (2), 742–755.
Shapira, A., 1981. Assessment of the potential earthquake risk in Israel and adjacent areas. Isr. J. Earth Sci. 30, 135–141.
Shapira, A., 1983. Aprobabilistic approach for evaluating earthquake risks with application to the Afro-Eurasian junction. Tectonophysics 91, 321–334.
Shapira, A., Fernández, L.M., 1989. Probabilities of exceedance for prescribed peak ground accelerations (PGA) at selected southern African locations. Tectonophysics 167, 253–260.
Shudofsky, G.N., 1985. Source mechanism and focal depths of East African earthquakes using Rayleigh-wave inversion and body-wave modelling. Geophys. J. R. Astron. Soc. 83, 563–614.
Singh, M., Kijko, A., Durrheim, R., 2009. Seismotectonic models for South Africa: Synthesis of geoscientific information, problems, and the way forward. Seismol. Res. Lett. 80 (1), 71–80.
Singh, M., Kijko, A., Durrheim, R., 2011. First-order regional seismotectonic model for South Africa. Nat. Hazards 59, 383–400.
Smit, L., Fagereng, Å., Braeuer, B., Stankiewicz, J., 2015. Microseismic activity and basement controls on an active intraplate strike-slip fault, Ceres-Tulbagh, South Africa. Bull. Seismol. Soc. Am. 105 (3), 1540–1547.
Spudich, P., Chiou, B.S., Graves, R.W., Collins, K.R., Somerville, P.G., 2004. A formulation of directivity for earthquake sources using isochrone theory. U.S. Geological Survey Open-File Report 2004- 1268, pp54.
Spudich, P., Chiou, B.S.J., 2008. Directivity in NGA earthquake ground motions: analysis using isochrone theory. Earthq. Spectra 24 (1), 279–298.
Strasser, F.O., Albini, P., Flint, N.S., Beauval, C., 2015. Twentieth century seismicity of the Koffiefontein region (Free State, South Africa): consistent determination of earthquake catalogue parameters from mixed data types. J. Seismol. 19, 915–934.
Terrier, M., Blès, J.L., Godefroy, P., Dominique, P., Bour, M., Martin, C., 2000. Zonation of Metropolitan France for the application of earthquake-resistant building regulations to critical facilities Part 1: seismotectonic zonation. J. Seismol. 4 (3), 215–230.
Theron, J.N., 1974. The seismic history of the south-western Cape province. In: Van Wyk, W.L., Kent, L.E. (Eds.), The Earthquake of 29 September 1969 in the South-Western Cape Province, South Africa, Seismological Series 4. Geological Survey of South Africa, pp. 9–16.
Tucholke, B.E., Houtz, R.E., Barrett, D.M., 1981. Continental crust beneath the Agulhas plateau, southwest Indian Ocean. J. Geophys. Res. 86, 3791–3806.
Turyomurugyendo, G., 1996. Some Aspects of Seismic Hazard in the East and South African Region. MSc Thesis. Institute of Solid Earth Physics, University of Bergen, Bergen, Norway.
Uenzelmann-Neben, G., Huhn, K., 2009. Sedimentary deposits on the southern South African continental margin: Slumping versus non-deposition or erosion by oceanic currents? Mar. Geol. 266, 65–79.
USNRC, 2012. Practical Implementation Guidelines For SSHAC Level 3 And 4 Hazard Studies. US Nuclear Regulatory Commission, pp. 235 Technical report.
Wagner, G.S., Langston, C.A., 1988. East African earthquake body wave inversion with implications for continental structure and deformation. Geophys. J. 94 (3), 503–518.
Wells, D.L., Coppersmith, K.J., 1994. New empirical relationships among magnitude, rupture length, rupture width, rupture area, and surface displacement. Bull. Seismol. Soc. Am. 84, 974–1002.
White, S., Stollhofen, H., Stanistreet, I.G., Lorenz, V., 2009. Pleistocene to recent rejuvenation of the Hebron fault, SW Namibia. Geological Society 316, 293–317 London, Special Publications.
Wiemer, S., 2001. A software Package to Analyze seismicity: ZMAP. Seismol. Res. Lett. 72, 374–383.